Research Square

Preprints are preliminary reports that have not undergone peer review.
They should not be considered conclusive, used to inform clinical practice,
or referenced by the media as validated information.

Dasatinib Alleviates Sepsis by Restoring Regulatory T Cell Homeostasis through the SRC/ADAM10/CD25 Axis

Jiahui Pan
School of Medical Technology, Guangdong Medical University
Junyi Shao
The First Dongguan Affiliated Hospital, Guangdong Medical University
Nianke Zang
Department of Immunology, School of Cell and Gene Therapy, Songjiang Research Institute, Shanghai Songjiang District Central Hospital, Shanghai Jiao Tong University School of Medicine
Jiafu Li
The First Dongguan Affiliated Hospital, Guangdong Medical University
Yuting Qin
The First Dongguan Affiliated Hospital, Guangdong Medical University
Yu Liu
The First Dongguan Affiliated Hospital, Guangdong Medical University
Jianbo Sun
The First Dongguan Affiliated Hospital, Guangdong Medical University
Wenhong Hou
The First Dongguan Affiliated Hospital, Guangdong Medical University
Songguo Zheng
Department of Immunology, School of Cell and Gene Therapy, Songjiang Research Institute, Shanghai Songjiang District Central Hospital, Shanghai Jiao Tong University School of Medicine
Yiming Shao
sym@gdmu.edu.cn

The First Dongguan Affiliated Hospital, Guangdong Medical University

Research Article

Keywords: Sepsis, SRC, ADAM10, Immune Dysregulation, Regulatory T Cells (Tregs)

Posted Date: November 14th, 2026

DOI: https://doi.org/10.21203/rs.3.rs-11343447/v1

License: This work is licensed under a Creative Commons Attribution 4.0 International License.
Read Full License

Additional Declarations: No competing interests reported.

Dasatinib Alleviates Sepsis by Restoring Regulatory T Cell Homeostasis through the SRC/ADAM10/CD25 Axis

Jiahui Pan · Junyi Shao · Nianke Zang · Jiafu Li · Yuting Qin · Yu Liu · Jianbo Sun · Wenhong Hou · Song Guo Zheng* · Yiming Shao*

* Corresponding author.

Abstract

Sepsis-induced immune paralysis, driven by regulatory T cell (Treg) reduction, is a major cause of mortality. While A Disintegrin and Metalloproteinase 10 (ADAM10) overactivation is observed in patients with sepsis, its precise upstream regulation and role in Treg dysfunction remain unclear. Bioinformatics and clinical data from sepsis patients revealed a significant inverse correlation between ADAM10 and Treg markers. Mechanistically, SRC (Steroid receptor coactivator) kinase directly interacted with and phosphorylated ADAM10, triggering its hyperactivity. This led to excessive shedding of surface CD25 (sCD25 release), which impaired the IL-2 signaling essential for Treg differentiation. The SRC inhibitor Dasatinib dose-dependently inhibited ADAM10, restored CD25 surface expression, and rescued Treg frequency. Critically, this restorative effect was abolished by an ADAM10 agonist, confirming the specificity of the SRC-ADAM10 pathway. In septic mice, Dasatinib treatment also significantly reduced plasma sCD25, increased splenic Tregs, attenuated organ injury, and improved survival. This study elucidates a novel SRC-ADAM10-CD25 axis driving Treg reduction in sepsis and identifies Dasatinib as a potential drug repurposing candidate to

restore immune homeostasis in patients with sepsis.

Keywords: Sepsis · SRC · ADAM10 · Immune Dysregulation · Regulatory T Cells (Tregs)

Introduction

Sepsis is a life-threatening condition characterized by organ dysfunction due to a dysregulated host response to infection [1]. It represents the leading cause of death in intensive care units (ICUs) worldwide and is associated with high rates of morbidity and mortality[2]. The pathogenesis of sepsis is highly complex, fundamentally defined by a biphasic immunopathological response. In this process, hyperinflammatory and immunosuppressive states can be activated synchronously, sequentially, or concurrently [3]. Excessive inflammation coupled with a profound disruption of immune homeostasis are key drivers of disease progression and poor patient outcomes. Patients typically present with an initial hyperinflammatory phase, characterized by a 'cytokine storm' and extensive immune cell infiltration [4]. Crucially, this inflammatory surge is often accompanied or immediately followed by signs of immune paralysis, a state of profound immunosuppression [5–7]. Consequently, all current experimental therapeutic strategies targeting sepsis-induced immune paralysis share a core objective: to reduce immune cell apoptosis and loss, enhance the recovery of immune cell populations, and restore their regenerative and functional capacity [8,9].

A Disintegrin and Metalloproteinases (ADAMs) are transmembrane proteins that regulate key cellular processes—including adhesion, migration, proteolysis, and signal transduction—through their metalloproteinase activity [10]. This activity enables immune and endothelial cells to cleave and release a wide range of substrates, such as inflammatory mediators, adhesion molecules, and chemokines [11–13]. In prior work,

we identified ADAM10 as playing a critical role in sepsis-associated endothelial injury. Under septic conditions, ADAM10 is markedly overexpressed and hyperactivated, with its expression and activity levels closely correlating with disease severity [14–17]. Interactome studies indicate that the cytoplasmic tail of ADAM10 can bind multiple adaptor proteins and non-receptor tyrosine kinases containing Src homology 3 (SH3) domains, notably members of the Src family kinases (SFKs) such as SRC, Fyn, and Lyn [18]. These interactions influence ADAM10 trafficking, localization, and enzymatic regulation [19]. Bioinformatics analyses further highlight SRC—a core SFK member—as a key regulatory factor in the pathogenesis of neonatal sepsis [20]. Although SRC has been shown to directly bind the cytoplasmic domain of ADAM10 in pituitary adenomas, thereby modulating cell proliferation and migration [21], and although ADAM10 activation *via* an SRC-dependent pathway has been reported in pemphigus vulgaris [22], the precise nature and regulatory consequences of the SRC-ADAM10 interaction in sepsis remain poorly understood and warrant further investigation.

Regulatory T cells (Tregs) are a specialized population of $CD4^+$ T lymphocytes essential for maintaining immune homeostasis [23,24]. Their core functions include suppressing excessive immune activation, sustaining immune tolerance, and preventing autoimmunity [25]. Evidence indicates that Tregs also play a pivotal role in adaptive immunity during sepsis. In the early inflammatory phase, they help restrain excessive inflammation, promote bacterial clearance, and mitigate tissue injury [26,27]. However,

clinical studies reveal a significant reduction in absolute Treg counts in patients with septic shock and in non-survivors of sepsis [28–31].

Nevertheless, the upstream mechanisms driving ADAM10 overactivation and their therapeutic potential remain unclear. Based on the established role of SRC in regulating ADAM10 and its identification as a sepsis-associated kinase, we hypothesized that Dasatinib—a clinically approved SRC-family kinase inhibitor—could be repurposed to block the SRC-ADAM10 axis. This inhibition would be expected to prevent pathological CD25 shedding and restore Treg homeostasis. To test this, we integrated clinical analysis, mechanistic rescue experiments, and *in vivo* sepsis models to validate the pathway and provide a translational foundation for immunotherapy in sepsis.

Materials and methods

Peripheral blood mononuclear cells purification and ethical use of human samples

Human peripheral blood mononuclear cells (PBMCs) were isolated from the peripheral blood of healthy volunteers and patients with sepsis. All experimental procedures involving human subjects were conducted in accordance with the ethical standards of the Declaration of Helsinki and were approved by the Medical Ethics Review Committee of Dongguan First Affiliated Hospital of Guangdong Medical University (Approval No. SLYJ202506001). Written informed consents were obtained from all individual participants included in this study.

Animals

Specific pathogen-free (SPF) male C57BL/6 mice, aged 5–9 weeks and weighing 20–25 (±0.4) g, were purchased from Beijing SPF Biotechnology Co., Ltd., and used in this study, which was performed exclusively in males to minimize confounding effects of estrous cycle-associated hormonal fluctuations on the inflammatory response to sepsis, a standard practice in cecal ligation and puncture (CLP) models. All mice were group-housed under controlled environmental conditions with a 12-hour light/dark cycle, a constant temperature of 22±2 °C, and a relative humidity of 40%-60%. All animal experimental protocols were approved by Shenzhen Top Biotech Co., Ltd. Institutional Animal Care and Use Committee, IACUC (TOP-2PZ-GM251208).

Establishment of cecal ligation and puncture (CLP) sepsis mouse model

Wild-type male C57BL/6 mice were fasted for 12 hours with free access to water before surgery. Mice were anesthetized to a deep anesthetic state *via* intraperitoneal injection of 2% pentobarbital sodium (50 mg/kg). After shaving and disinfecting the abdominal area, a midline abdominal incision (1–1.5 cm in length) was made, and the cecum was exposed from the left lower abdomen. The cecum was ligated 0.5 cm below the ileocecal valve and punctured once back and forth with a 23-gauge needle (2.6 × 65 mm). The cecum was gently squeezed to extrude a small amount of feces, then carefully returned to the abdominal cavity, and the abdominal wall and skin incisions were sutured layer by layer. The surgical wound was disinfected with iodine tincture. Each mouse was administered resuscitation fluid (0.9% NaCl, 37 °C, 50 mL/kg) *via*

subcutaneous injection. After anesthesia recovery, mice were allowed free access to food and water. Postoperatively, the mice were closely monitored for sepsis-related symptoms, including mental status, food and water intake, respiratory rate, fur condition, stool characteristics, body temperature changes, and skin temperature.

Western blotting

Cell samples were centrifuged at 500 *g*. The supernatant was discarded, and the cell pellet was lysed in RIPA lysis buffer containing protease inhibitors for 30 min on ice. The protein concentration of each sample was normalized according to the instructions of the BCA Protein Assay Kit. Protein samples were separated by SDS-PAGE at 80 V for 30 min until the sample front entered the separating gel, followed by electrophoresis at 120 V for 60 min. Proteins were transferred onto PVDF membranes at 400 mA for 35 min. The membranes were blocked with protein-free rapid blocking buffer for 30 min at room temperature, then incubated with primary antibodies at 4 °C overnight. After washing with TBST, the membranes were incubated with secondary antibodies for 1 h at room temperature. Protein bands were visualized using an automated chemiluminescence imaging system (Tanon 5200, Shanghai, China) and quantified using ImageJ software.

Flow cytometry analysis

Cells were collected and centrifuged at 500 *g* at 4 °C for 5 min. The antibodies used were as follows: Brilliant Violet 510 CD45 (clone 30-F11; BD Pharmingen), Alexa

Fluor 700 CD3 (clone 500A2; BD Pharmingen), Brilliant Violet 786 CD4 (clone GK1.5; BD Pharmingen), PerCP-Cyanine5.5 CD8a (clone 53－6.7; BD Pharmingen), APC CD44 (clone IM7; BD Pharmingen), CD62L (clone MEL-14; BD Pharmingen), BD Horizon Brilliant Blue 515 CD25 (clone PC61; BD Pharmingen), PE-Cyanine7PE IFN-γ (clone XMG1.2; BD Pharmingen) and Brilliant Violet 650 IL-17 A (clone TC11-18H10; BD Pharmingen). For Tregs staining, cells stained with surface molecules were fixed, permeabilized, and stained intracellularly with Foxp3 using the Transcription Factor Buffer kit (BD Pharmingen) according to the manufacturer's directions. Finally, cells were washed three times, fixed with 0.5% paraformaldehyde, and then analyzed on BD FACS Aria III (BD Biosciences, San Jose, CA, USA).

In vitro sorting and induction of naïve $CD4^+$ T cells

Spleens were harvested from C57BL/6J mice, and single-cell suspensions were prepared and centrifuged. The cell pellet was resuspended in red blood cell lysis buffer for 1 min, then neutralized with 6− 8 mL of culture medium containing 10% fetal bovine serum (FBS) or PBS, followed by centrifugation to discard the supernatant. The cell pellet was stained with PE-conjugated anti-CD4 and APC-conjugated anti-CD62L antibodies at 4 °C for 30 min in the dark, and naïve $CD4^+$ T cells were sorted using a flow cytometer. After sorting, 0.5 million cells were re-analyzed by flow cytometry to verify the sorting efficiency. Two hours prior to cell culture, 96-well plates were coated with PBS containing 1 μg/mL Ultra-LEAF™ Purified anti-mouse CD3ε antibody. After discarding the coating solution, the wells were filled with RPMI 1640 medium

supplemented with 1 μg/mL Ultra-LEAF™ Purified anti-mouse CD28 antibody, 50 U/mL IL-2, and 4 ng/mL TGF-β as we previously described.[32] The sorted naïve $CD4^+$ T cells were seeded into the coated wells at a density of 5×10^5 cells per well, and cultured in a 37 °C incubator with 5% CO_2 for 3 d.

Hematoxylin-Eosin (HE) staining

Mouse tissue samples were harvested and fixed in paraformaldehyde for 24 h. The fixed tissues were dehydrated through a graded ethanol series (70%, 80%, 90%, 95%, and 100%) for 1−2 h per step, then embedded in molten paraffin and allowed to solidify. Paraffin blocks were sectioned into 4−6 μm thick slices, which were flattened in a 40 °C water bath, mounted onto glass slides, and dried. The sections were stained with HE, sealed with neutral gum and coverslips, and air-dried. Tissue pathological sections were scanned and imaged using a digital pathological slide scanner, and tissue damage was scored. Lung tissue damage was evaluated based on indicators including pulmonary edema, hyaline membrane formation, hemorrhage, atelectasis, and inflammatory cell infiltration. Renal tissue damage was assessed by vacuolar degeneration, renal tubular epithelial edema, tubular atrophy, necrosis, and exfoliation. A 1−4 points scoring system was used to determine the severity of lesions, with the total pathological score calculated by summing the scores of each area based on the percentage of affected area.

Immunofluorescence staining

A square was marked on an immunofluorescence slide using an immunofluorescence pen, and cells were fixed by adding 200 μL of 4% PFA dropwise into the square. The slide was blocked with immunostaining blocking buffer for 30 min− 1 h at room temperature, then washed 3− 5 times with 200 μL of PBS. SRC and ADAM10-specific polyclonal antibodies were diluted to the appropriate concentration, and the diluted primary antibody solution was gently added to the cell area on the slide to ensure full coverage of the cells. The slide was incubated overnight at 4 °C on a shaker, then washed 3− 5 times with PBS. The cells were incubated with Alexa Fluor 647-conjugated goat anti-rabbit IgG and Cyanine 3-conjugated goat anti-mouse IgG at 4 °C for 1− 2 h in the dark. After recovering the secondary antibodies, the slide was washed 3− 5 times with 200 μL of PBS, and finally mounted with 20 μL of anti-fluorescence quenching mounting medium containing DAPI. The slides were scanned and imaged using a digital pathological slide scanner, and the images were analyzed using ImageJ software.

Enzyme-linked immunosorbent assay (ELISA)

The mouse enzyme-linked immunosorbent assay (ELISA) kit was used to quantitatively detect the level of soluble CD25 (sCD25) in mouse plasma in strict accordance with the kit instructions, and the absorbance value of each sample was measured using an iMark microplate reader.

Statistical analysis

All experimental data were statistically analyzed and graphed using GraphPad Prism software (Version 8.0, GraphPad Software, USA). Quantitative data were presented as mean ± standard deviation (mean ± SD). For normally distributed data, independent sample t-tests were used for comparisons between groups; for non-normally distributed data, Mann-Whitney U tests were applied. Chi-square tests were used for the analysis of categorical data. A P-value < 0.05 was considered statistically significant.

Results

Elevated ADAM10 expression and decreased Treg cell frequency are present in both septic patients and mouse models

To clarify the potential role of ADAM10 in sepsis-associated immune dysregulation, we first analyzed clinical transcriptomic datasets to characterize the expression patterns of ADAM10 and Treg-related molecules under septic conditions. Transcriptomic analysis revealed that, compared with healthy controls, ADAM10 mRNA expression was significantly upregulated in peripheral blood mononuclear cells (PBMCs) from septic patients. In contrast, the transcription levels of Treg-associated genes, including FOXP3, IL2RA, and STAT5, were markedly downregulated, whereas the pro-inflammatory cytokine IL-6 was significantly increased (Fig. 1A). Correlation analysis further demonstrated that ADAM10 expression was significantly and negatively correlated with FOXP3, IL2RA, and STAT5, but positively correlated with IL-6, indicating that aberrant ADAM10 expression is closely associated with Treg

dysfunction and inflammatory imbalance in sepsis (Fig. 1B).

To validate these transcriptomic findings at the protein level, flow cytometric analyses were performed on clinical PBMC samples. The results showed that the proportions of $CD4^+$ $CD25^+$ T cells and $CD4^+$ $FOXP3^+$ Tregs were significantly reduced in septic patients compared with healthy controls, indicating a pronounced reduction of Tregs during sepsis (Fig. 1C). Meanwhile, ADAM10 protein expression in PBMCs from septic patients was markedly increased, as evidenced by a rightward shift of fluorescence intensity peaks and a significant elevation of mean fluorescence intensity (MFI) (Fig. 1D). Consistently, Western blot analysis further confirmed that ADAM10 protein levels were significantly higher in the sepsis group than that in healthy controls based on quantitative densitometric analysis (Fig. 1E).

To extend these clinical observations to an experimental model, a cecal ligation and puncture (CLP) mouse model of sepsis was established, and splenocytes were analyzed. Flow cytometric analysis recapitulated the clinical findings: compared with sham controls, CLP mice exhibited significantly reduced proportions of $CD4^+$ $CD25^+$ T cells and $CD4^+$ $FOXP3^+$ Tregs in splenic tissues (Fig. 1F). In line with the human data, both MFI analysis by flow cytometry and Western blot results demonstrated a significant upregulation of ADAM10 protein expression in splenic T cells from CLP mice, further validating the sepsis-associated ADAM10 high-expression phenotype (Fig. 1G-H).

Collectively, these data demonstrate that both septic patients and sepsis mouse models exhibit pronounced Treg decrease accompanied by synchronous upregulation of ADAM10 in lymphocytes, suggesting a potential mechanistic link between ADAM10

dysregulation, Treg impairment, and immune imbalance in sepsis.

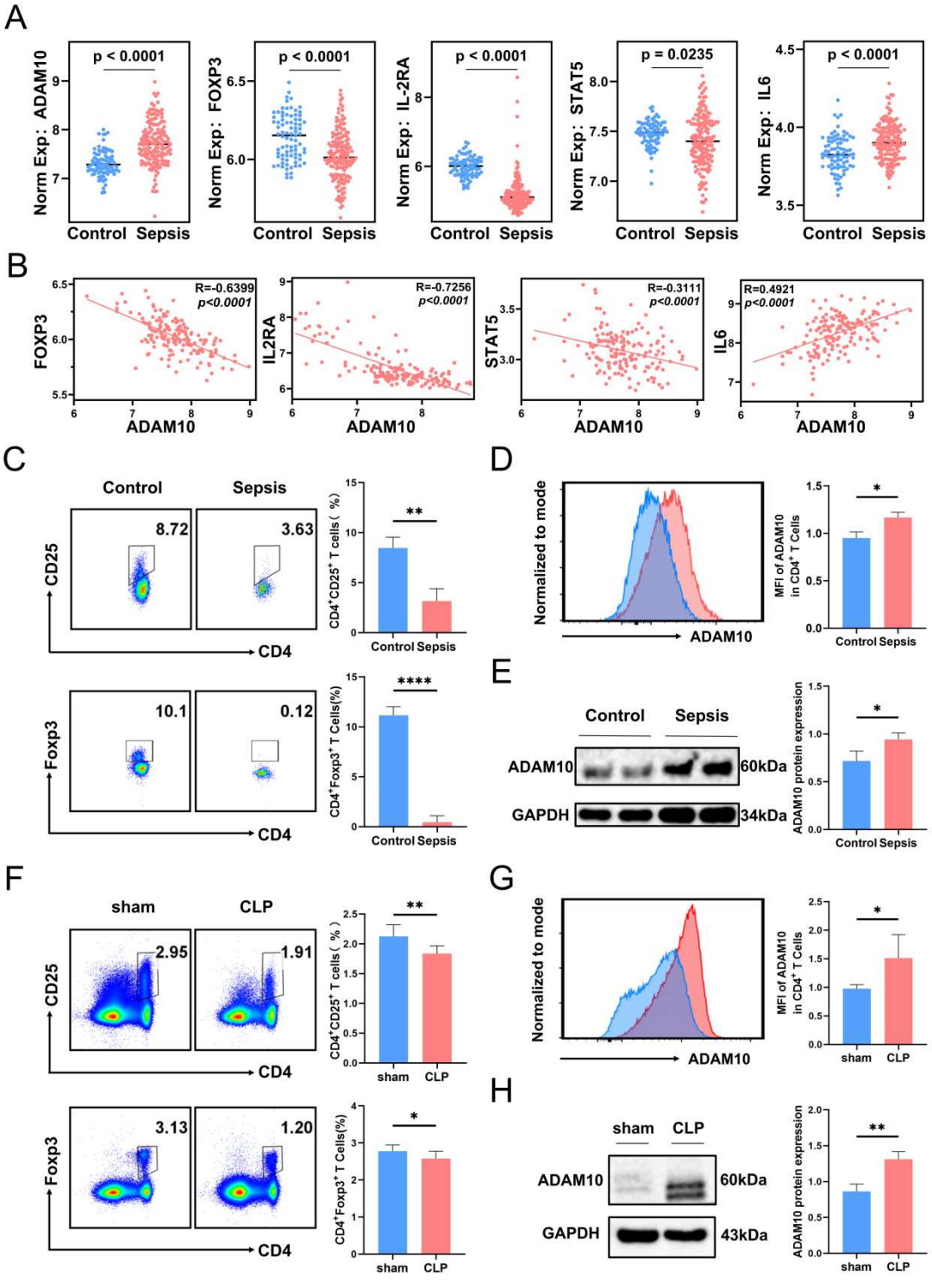


Figure. 1 ADAM10 is upregulated in sepsis and associated with altered Tregs-related signaling. (**A**) Scatter plots visualizing the distribution of transcriptional expression levels of ADAM10, FOXP3, IL2RA, STAT5, and IL6 in peripheral blood mononuclear cells (PBMCs) from healthy

controls and sepsis patients in the GSE134347 dataset. (**B**) Correlation scatter plots with fitted lines, demonstrating the association of ADAM10 transcriptional levels with FOXP3, IL2RA, STAT5, and IL6 in PBMCs of sepsis patients via Pearson correlation analysis. (**C**) Flow cytometry (left) and histogram analysis (right) were performed to detect the proportions of $CD4^+$ $CD25^+$ T cells and $CD4^+$ $FOXP3^+$ Tregs in PBMCs from healthy controls and sepsis patients. (**D**) Flow cytometry (left) and histogram analysis (right) were applied to determine the mean fluorescence intensity (MFI) of ADAM10 in PBMCs from the above two groups. (**E**) Western blot (left) and histogram analysis (right) were used to examine the expression level of ADAM10 protein in PBMCs from healthy controls and sepsis patients. (**F**) Flow cytometry (left) and histogram analysis (right) were conducted to analyze the proportions of $CD4^+$ $CD25^+$ T cells and $CD4^+$ $FOXP3^+$ Tregs in the spleen tissues of mice from the sham group and cecal ligation and puncture (CLP) group at 12 h post-operation. (**G**) Flow cytometry (left) and histogram analysis (right) were employed to detect the MFI of ADAM10 in the spleen tissues of mice from the sham group and CLP group. (**H**) Western blot (left) and histogram analysis (right) were utilized to measure the expression level of ADAM10 protein in splenocytes from the sham group and CLP group. Data were presented as mean ± SEM from at least three independent experiments. $*P < 0.05$, $**P < 0.01$, $***P < 0.001$, $****P < 0.0001$.

ADAM10 hyperactivation impairs Treg differentiation *via* proteolytic cleavage of surface CD25

To investigate whether ADAM10-mediated CD25(IL-2Rα) cleavage impairs Tregs generation, we differentiated induced Tregs (iTregs) *in vitro* under LPS-simulated

274 septic conditions in the presence or absence of the ADAM10 inhibitor GI254023X.
275 Quantification confirmed a significant LPS-induced increase in ADAM10 MFI, which
276 was effectively reduced by the inhibitor (Fig. 2A). Consistent with enhanced
277 ectodomain shedding, ELISA measurement of culture supernatants showed that LPS
278 stimulation significantly elevated soluble CD25 (sCD25) levels. This increase was
279 markedly suppressed by GI254023X, confirming that ADAM10 activity is responsible
280 for the pathological release of sCD25 under these conditions (Fig. 2B). Analysis of Treg
281 populations demonstrated that LPS stimulation significantly reduced the proportions of
282 both $CD4^+$ $CD25^+$ T cells and $CD4^+$ $FOXP3^+$ Tregs compared to PBS controls.
283 Inhibition of ADAM10 with GI254023X restored these frequencies to near-baseline
284 levels (Fig. 2C). Together, these findings indicate that ADAM10-mediated proteolytic
285 cleavage of surface CD25, evidenced by increased sCD25 release, is a key mechanism
286 impairing Treg generation *in vitro* during LPS-simulated sepsis. Pharmacological
287 inhibition of ADAM10 preserved membrane CD25 expression, mitigated functional
288 impairment, and restored Treg differentiation, identifying ADAM10 as a critical
289 regulator of Treg homeostasis *via* CD25 shedding.

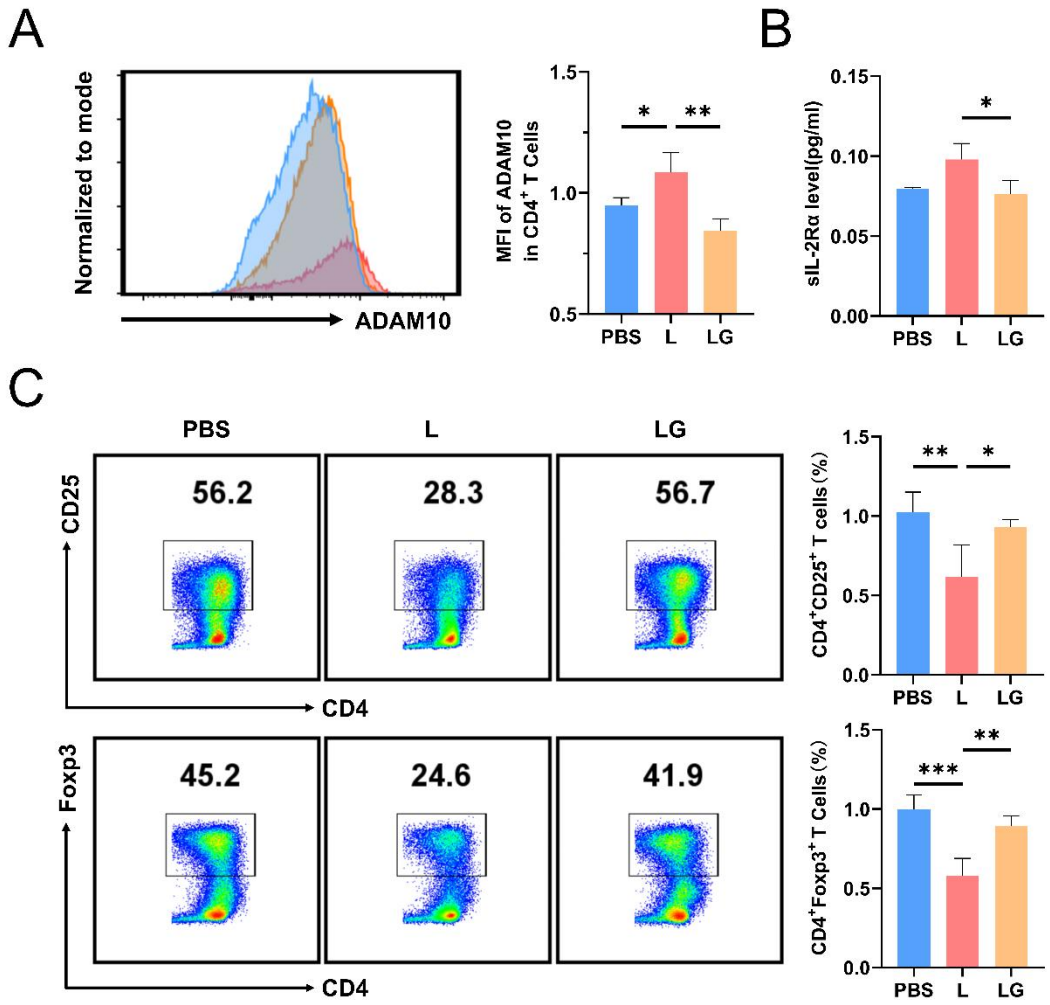


Figure. 2 ADAM10-mediated cleavage of IL-2Rα regulates downstream Tregs generation. (**A**) Flow cytometry (left) and histogram analysis (right) were used to examine the MFI of ADAM10 in $CD4^+$ T cells. (**B**) Enzyme-linked immunosorbent assay (ELISA) was employed to measure the concentrations of soluble interleukin-2 receptor α (sIL-2Rα) in culture supernatants, and the resulting data were statistically analyzed using histograms. (**C**) Flow cytometry (left) and histogram analysis (right) were employed to analyze the proportions of $CD4^+$ $CD25^+$ T cells and $CD4^+$ $Foxp3^+$ Tregs. Abbreviations: L, lipopolysaccharide (LPS); LG, LPS + ADAM10 inhibitor GI254023X (G). Data were presented as mean ± SEM from at least three independent experiments. *$P < 0.05$, **$P < 0.01$, ***$P < 0.001$, ****$P < 0.0001$.

SRC kinase acts as an upstream activator of ADAM10 through direct interaction and phosphorylation

To elucidate the molecular mechanism underlying SRC-mediated regulation of ADAM10, we systematically investigated their physical interaction, expression correlation, and functional dependency in sepsis models. First, we performed co-immunoprecipitation (co-IP) assays to test the direct interaction between SRC and ADAM10. when cell lysates were immunoprecipitated with an anti-SRC antibody, ADAM10 was readily detected in the precipitated complex. In contrast, no ADAM10 signal was observed in the IgG control group, confirming the specific physical association between SRC and ADAM10 in cells (Fig. 3A). We next assessed the functional dependency of ADAM10 on SRC activity. Treatment with increasing concentrations of the SRC inhibitor Dasatinib prior to LPS stimulation resulted in a dose-dependent decrease in ADAM10 protein levels. Notably, inhibition of ADAM10's metalloprotease activity with GI254023X similarly reduced ADAM10 protein abundance, suggesting that SRC signaling is required for maintaining ADAM10 expression in this context (Fig. 3B). Immunofluorescence staining provided direct evidence of a molecular interaction, showing distinct co-localization of p-SRC (red) and ADAM10 (green) signals within the cytoplasm of septic cells (Fig. 3C). This regulatory axis was further validated in primary $CD4^+$ T cells. Dasatinib treatment induced a dose-dependent reduction in ADAM10 protein levels as measured by western blot (Fig. 3D). Consistent with this, flow cytometric analysis confirmed a significant

decrease in ADAM10 mean fluorescence intensity (MFI) in primary $CD4^+$ T cells treated with Dasatinib (Fig. 3E). Collectively, these data demonstrate that SRC kinase activity is required for ADAM10 upregulation in sepsis. The observed co-localization, coupled with the loss of ADAM10 expression upon SRC inhibition, establishes SRC as a direct upstream regulator controlling ADAM10 levels in immune cells during septic insult.

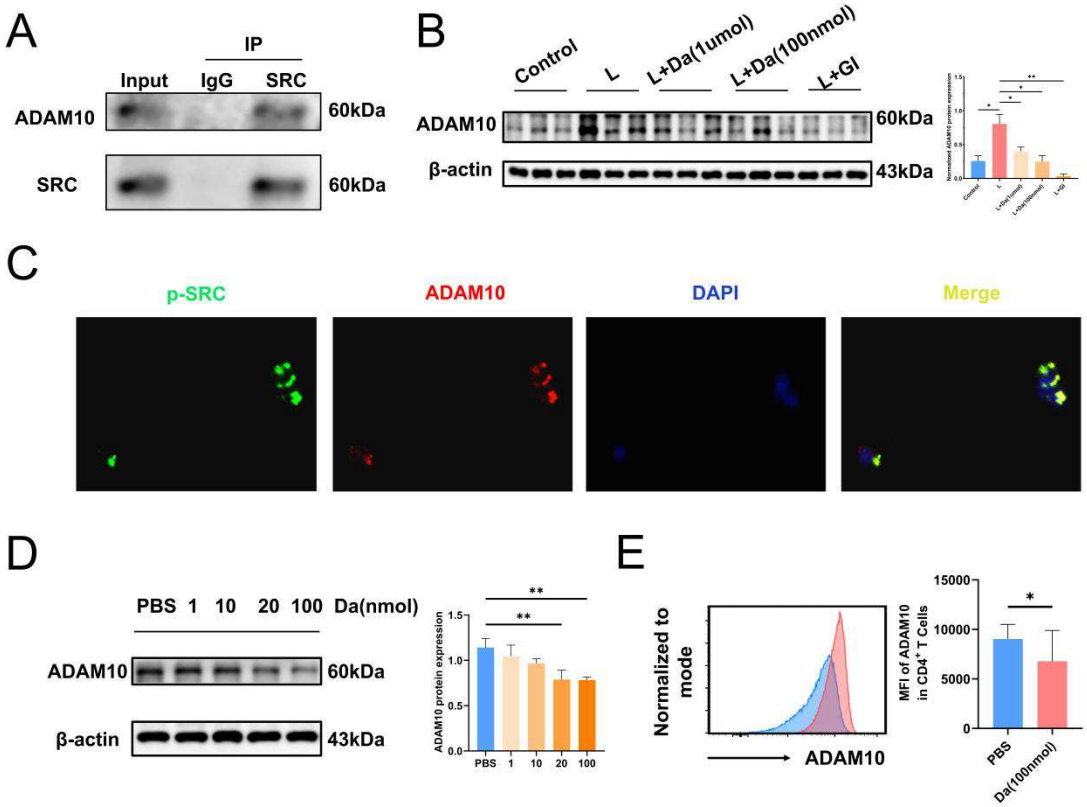


Figure. 3 SRC activation mediates ADAM10 expression. (**A**) Immunoprecipitation using anti-SRC antibody confirmed the interaction between SRC and ADAM10. IgG was used as a negative control. (**B**) Western blot (left) and histogram analysis (right) were employed to analyze the protein expression level of ADAM10 in $CD4^+$ T cells from the control group, LPS-treated group (1 μg/mL), SRC inhibitor Dasatinib-treated groups (1 μmol/L or 100 nmol/L) and ADAM10 inhibitor GI254023X-treated group (10 μmol/L). (**C**) Fluorescence microscopy observation of

phosphorylated SRC (p-SRC, green, Cy3), ADAM10 (red, AF647), and cell nuclei (blue, DAPI) in Tregs cells. Merged images were presented as composite images integrating the green, red, and blue channels. Scale bar = 20 μm. (**D**) Western blot (left) and histogram analysis (right) were used to determine the protein expression level of ADAM10 in Jurkat cells following 12-hour incubation with PBS or different concentrations of SRC inhibitor decitabine (1, 10, 20 or 100 nmol/L). (**E**) Flow cytometry (left) and histogram analysis (right) were applied to detect the MFI of ADAM10 in Jurkat cells. Data were presented as mean ± SEM from at least three independent experiments. **P* < 0.05, ***P* < 0.01, ****P* < 0.001, *****P* < 0.0001.

ADAM10 activation abolishes the restorative effect of SRC inhibition, confirming the SRC-ADAM10-Treg axis

To definitively confirm that SRC regulates Treg homeostasis exclusively *via* ADAM10, we performed a drug intervention rescue experiment: naive $CD4^+$ T cells were cultured under LPS-induced sepsis-like differentiation conditions and treated with the SRC inhibitor dasatinib (D), with or without concurrent administration of an ADAM10 agonist (I). Analysis of CD25 expression showed that LPS treatment alone significantly reduced the proportion of $CD4^+$ $CD25^+$ T cells and CD25 MFI (Fig. 4A). In contrast, combined treatment with dasatinib (Group L+D) not only effectively restored the LPS-induced loss of $CD4^+$ $CD25^+$ T cells but also significantly increased CD25 MFI, accompanied by a marked elevation in ADAM10 MFI. Notably, the concurrent addition of the ADAM10 agonist (Group L+D+I) completely abrogated the restorative effects

of dasatinib: both the proportion of $CD25^+$ cells and CD25 MFI were reduced to levels comparable to those in the LPS-only group, and ADAM10 MFI also decreased accordingly.

This regulatory pattern was precisely recapitulated in Treg differentiation (Fig. 4B): LPS treatment suppressed the generation of $CD4^+$ $FOXP3^+$ Tregs and decreased FOXP3 MFI. Dasatinib treatment (Group L+D) restored both the LPS-impaired Treg proportion and FOXP3 MFI, and also induced a significant increase in ADAM10 MFI. However, reactivation of ADAM10 with its agonist (Group L+D+I) completely reversed this restoration: the Treg proportion was reduced to 64.9%, FOXP3 MFI dropped even below the level of Dasatinib monotherapy, and ADAM10 MFI also decreased correspondingly.

Taken together, the restorative effects of SRC inhibition on CD25 expression and Treg differentiation are entirely dependent on the inhibition of ADAM10. The ability of the ADAM10 agonist to completely abolish the benefits of Dasatinib, coupled with the dynamic changes in ADAM10 MFI, provides definitive mechanistic evidence that SRC primarily regulates Treg homeostasis by activating the ADAM10-CD25 axis.

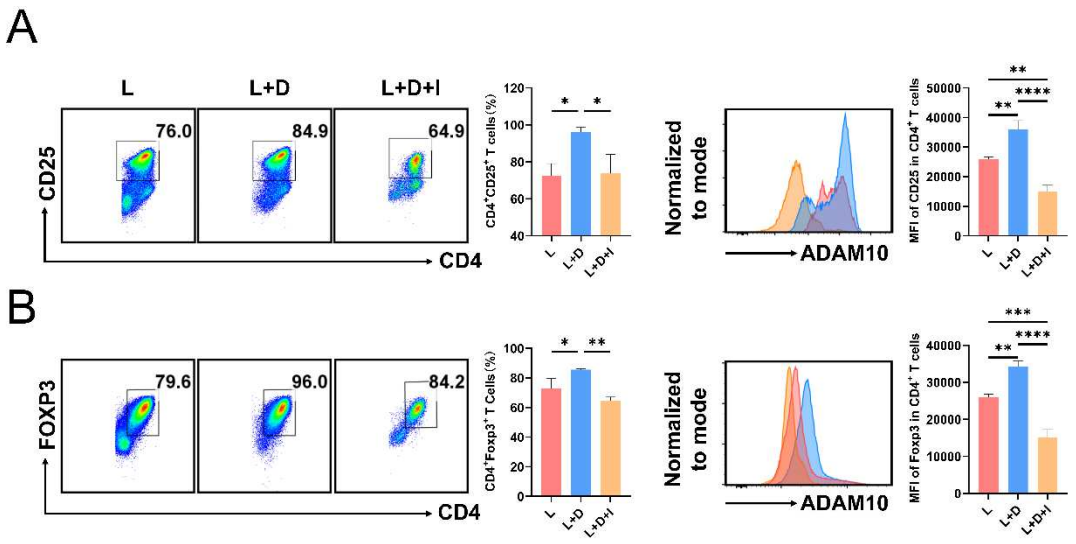


Figure. 4 Dasatinib restores Tregs homeostasis by blocking the SRC/ADAM10 signaling axis. (**A**) Flow cytometry (left) and quantitative histogram analysis (middle) were used to examine the proportions of $CD4^+$ $CD25^+$ T cells in the L, L+D, and L+D+I groups, and histograms (right) were employed to illustrate the changes in mean fluorescence intensity (MFI) of ADAM10 across these groups. (**B**) The same analytical approach was applied to determine the proportions of $CD4^+$ $Foxp3^+$ Tregs in the three groups, with concurrent presentation of ADAM10 MFI changes. Representative flow cytometry plots, quantitative analyses, and MFI statistics for ADAM10 are shown in the figures. Abbreviations: L, lipopolysaccharide (LPS); L+D, LPS + SRC inhibitor dasatinib; L+D+I, LPS + dasatinib + ADAM10 agonist IO Data are presented as mean ± SEM from at least three independent experiments. *$P < 0.05$, **$P < 0.01$, ***$P < 0.001$, ****$P < 0.0001$.

Dasatinib treatment restores Treg homeostasis and improves survival in sepsis by selectively targeting CD25 shedding

To determine whether the beneficial effects of Dasatinib in sepsis are mediated through

the restoration of Tregs, we evaluated the therapeutic efficacy of Dasatinib in a CLP model. Mice were administered Dasatinib 30 minutes before CLP surgery and again 6 hours postoperatively (Fig. 5A). Dasatinib treatment significantly reduced ADAM10 expression in splenic $CD4^+$ T cells of septic mice, as evidenced by a leftward shift in fluorescence intensity and a decrease in MFI compared with DMSO-treated CLP controls (Fig. 5B). This intervention conferred a significant survival advantage, with over 50% of Dasatinib-treated mice surviving beyond 60 hours, whereas all DMSO-treated CLP mice died within 40 hours (Fig. 5C). ELISA analysis of plasma revealed that Dasatinib specifically and significantly reduced levels of soluble CD25 (the cleaved ectodomain of IL-2Rα), without affecting concentrations of soluble IL-2Rβ or IL-2Rγ subunits (Fig. 5D). Flow cytometric analysis of splenocytes demonstrated that frequencies of $CD4^+$ $CD25^+$ and $CD4^+$ $FOXP3^+$ T cells were significantly higher in Dasatinib-treated CLP mice compared with CLP controls (Fig. 5E). These findings confirm the specific selectivity of the SRC-ADAM10 axis for CD25 shedding during sepsis.

Restoration of immune homeostasis was associated with significantly attenuated end-organ injury. Histopathological assessment showed that Dasatinib treatment significantly alleviated lung injury (reduced alveolar edema, inflammation, and hemorrhage) and renal injury (reduced tubular damage and inflammation) compared with sepsis controls, as quantified by blinded injury scoring (Fig. 5E–F). Collectively, these *in vivo* results demonstrate that SRC inhibition by Dasatinib suppresses ADAM10 activity, specifically attenuates CD25 shedding, rescues Treg deficiency, and ultimately

improves survival and organ function in experimental sepsis.

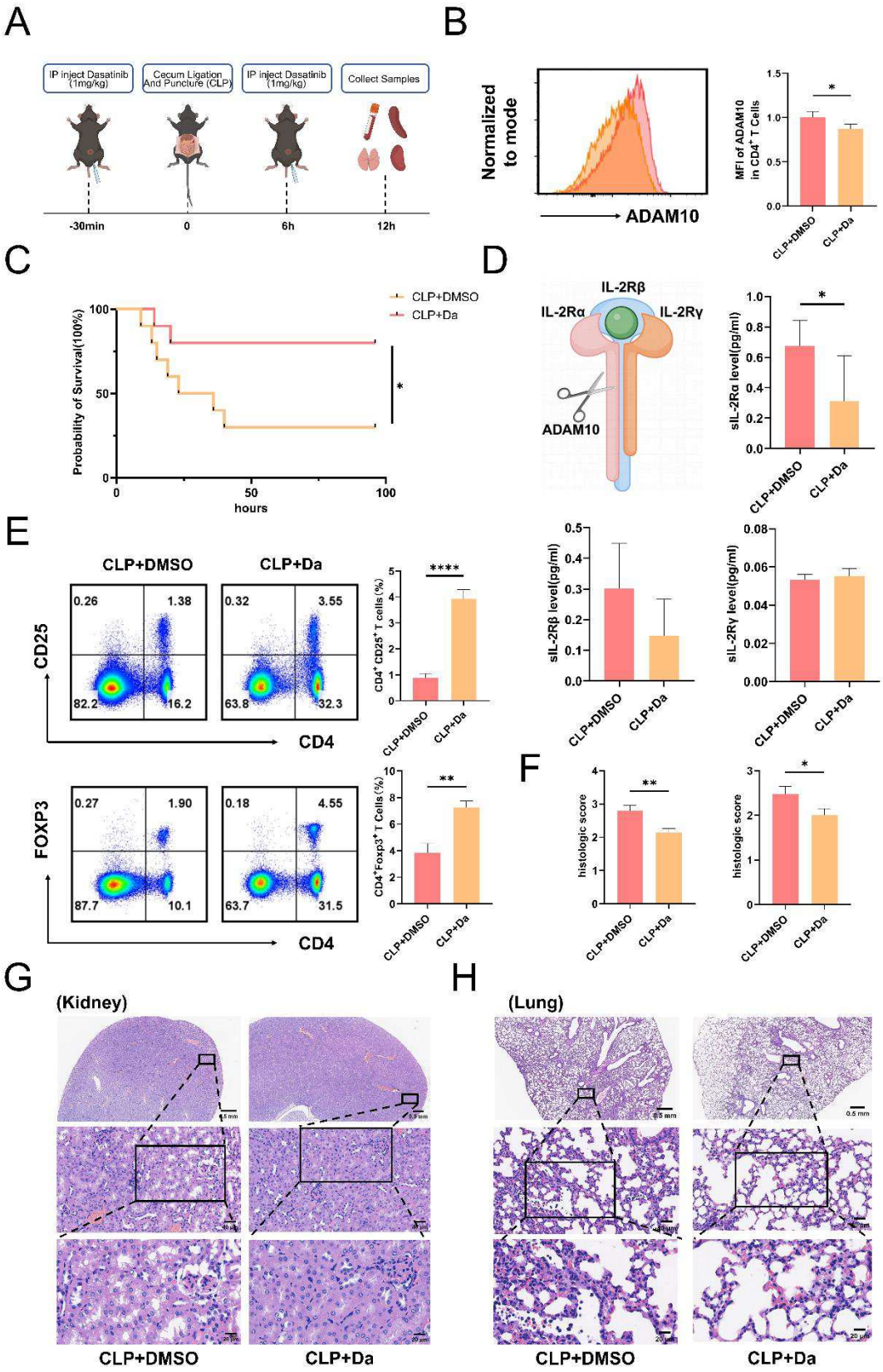


Figure. 5 SRC exacerbates immune disorders in septic mice by activating ADAM10. (**A**)

Experimental design: Wild-type male C57BL/6 mice were randomly assigned to the CLP group or the CLP + SRC inhibitor Dasatinib group. Dasatinib (1 mg/kg) was administered 30 minutes before surgery and 6 hours after CLP, and samples were collected 12 hours following the first dose. (**B**) Flow cytometry and histogram analysis were performed to detect the MFI of ADAM10 in splenic $CD4^+$ T cells of mice. (**C**) Survival rates of mice in each group were compared and analyzed. (**D**) A schematic diagram illustrates the hypothetical mechanism of ADAM10-mediated IL-2 receptor cleavage; concurrently, ELISA was used to measure serum levels of soluble IL-2Rα, IL-2Rβ, and IL-2Rγ. (**E**) Flow cytometry (left) and histogram analysis (right) were employed to evaluate the proportions of $CD4^+$ $CD25^+$ T cells and $CD4^+$ $Foxp3^+$ Tregs in the spleens of mice from the CLP group and CLP + Dasatinib group. (**F**) Quantitative analysis of histopathological injury scores in kidney and lung tissues was performed using histograms. (**G, H**) Representative HE-stained sections of kidney (G) and lung (H) tissues from each group are presented. Scale bars: upper row, 1.25 mm; middle row, 100 μm; lower row, 50 μm. Data are presented as mean ± SEM from at least three independent experiments. $*P < 0.05$, $**P < 0.01$, $***P < 0.001$, $****P < 0.0001$.

Discussion

Sepsis is defined by profound immune dysregulation, classically presenting as a biphasic response: an initial hyperinflammatory state followed by a period of immunosuppression [33]. The acute hyperinflammatory phase, driven by pathogen- and damage-associated molecular patterns (PAMPs/DAMPs) *via* pattern recognition receptors (PRRs), is characterized by a cytokine storm involving TNF-α, IL-1β, IL-6, and others, leading to clinical manifestations such as fever, shock, and organ failure

[34–36]. While this response is essential for pathogen clearance, its dysregulation causes collateral tissue damage and accelerates disease progression [37]. Regulatory T cells (Tregs), a specialized $CD4^+$ T cell subset, are critical for maintaining immune homeostasis by suppressing excessive or pathological responses [38]. They function through multiple mechanisms,, including cell-contact inhibition, secretion of anti-inflammatory cytokines (e.g., IL-10, TGF-β), and direct cytolysis [39–43]. In sepsis, Tregs help restrain early inflammation and mitigate tissue injury [27]. However, Treg deficiency is a hallmark of sepsis and other inflammatory diseases, contributing to immune paralysis [44–47]. As an IL-2-dependent population, Treg survival hinges on high-affinity IL-2 signaling *via* the CD25 receptor (IL-2Rα) [48,49], whereas low dose of IL-2 is also crucial for Treg induction and expansion [50–52]. Our study elucidates a novel mechanism for Treg loss in sepsis: ADAM10-mediated proteolytic cleavage of surface CD25, which disrupts this vital survival signal.

ADAM10 activity is tightly controlled by post-translational modifications and protein-protein interactions. Stimuli such as those in sepsis can rapidly activate ADAM10, often involving its recruitment to specific membrane microdomains [53,54]. Key regulators are proteins containing Src homology 3 (SH3) domains, which bind to proline-rich motifs on the ADAM10 cytoplasmic tail to modulate its trafficking and activity [55,56]. For instance, the kinase SRC, which contains an SH3 domain, can direct ADAM10 localization within lipid rafts, thereby influencing substrate specificity [57]. Prior work has shown that the phosphatase PP2A promotes Treg generation by inhibiting ADAM10

[58]. Conversely, we demonstrate that SRC kinase activates ADAM10, leading to CD25 shedding and subsequent Treg depletion, thereby exacerbating septic pathogenesis.

Dasatinib, an FDA-approved SRC-family kinase inhibitor used in leukemia [59,60], has documented immunomodulatory effects, including attenuation of TNF-α production and lung injury in inflammatory models [61,62]. We therefore investigated its potential to restore immune balance in sepsis. Our findings confirm that Dasatinib suppresses the SRC-ADAM10 axis, prevents CD25 cleavage, and rescues Treg differentiation and function *in vitro* and *in vivo*. In the CLP model, Dasatinib treatment improved survival, reduced organ injury, and specifically lowered plasma soluble CD25 levels without affecting other IL-2 receptor subunits, highlighting the pathway's selectivity.

This study provides several key advancements. First, it identifies SRC-dependent phosphorylation as a critical post-translational mechanism activating ADAM10 in sepsis, addressing a significant gap in understanding its upstream regulation. Second, it establishes a novel link between a central kinase signaling pathway (SRC) and adaptive immune regulation (Treg homeostasis), revealing important cross-talk within the septic immune microenvironment. Our work aligns with and extends recent insights into Treg fragility, including the roles of FOXP3 and mitochondrial regulators like Mcl-1 in Treg survival [63,64].

From a translational perspective, our data support the concept of drug repurposing for sepsis immunotherapy. Dasatinib, by specifically inhibiting the SRC-ADAM10 axis, offers a targeted strategy to restore the ‘immune brake’(Tregs) lost during sepsis. This approach of preventing a key receptor's shedding contrasts with broad immunosuppression and may help recalibrate the dysregulated immune response. Translating these findings to the clinic requires careful consideration of dosing and safety. The Dasatinib dosage used in our murine CLP model (1 mg/kg) approximates a human equivalent dose (HED) of 81 μg/kg, calculated based on body surface area, which falls within the range of doses used clinically for chronic myeloid leukemia. However, sepsis presents a distinct and dynamic pathophysiology. The profound immune dysregulation and frequent organ dysfunction in septic patients necessitate a rigorous re-evaluation of the risk-benefit profile. Known side effects of Dasatinib, such as pleural effusion, immunosuppression, and potential myelosuppression, could be exacerbated in the critical care setting. Therefore, future preclinical studies must establish an optimal therapeutic window for sepsis, balancing immunomodulatory efficacy with toxicity. Initial clinical exploration might involve lower doses or shortened treatment courses compared to oncology protocols, with stringent monitoring for infection control and organ function.

Our study is subject to several important limitations. First, although immunofluorescence suggests an association, direct evidence of a physical interaction between SRC and ADAM10—such as co-immunoprecipitation—and the mapping of

specific phosphorylation sites on ADAM10 by SRC are required to fully substantiate the proposed regulatory mechanism. Second, the functional consequences of the SRC-ADAM10 axis were examined primarily in Tregs. Its effects on other immune cell subsets and their potential crosstalk with Tregs in the septic microenvironment remain unexplored. Third, the clinical correlation data presented are cross-sectional. Longitudinal studies tracking the dynamics of this axis throughout the course of sepsis and recovery are needed to establish its prognostic or monitoring utility. Two further limitations warrant specific emphasis. First, while the pharmacological rescue experiment with an ADAM10 agonist strongly implicates the pathway, definitive genetic evidence—such as from T cell-conditional SRC or ADAM10 knockout models—is absent. Such approaches would conclusively demonstrate the cell-autonomous necessity of this axis in sepsis-induced Treg depletion. Second, and most critically for translational relevance, all interventional efficacy data originate from preclinical murine models. The profound complexity of human sepsis, encompassing diverse comorbidities, ages, pathogens, and immune histories, cannot be fully replicated in mice. Consequently, the therapeutic potential and safety of targeting the SRC-ADAM10 axis in septic patients remain to be established in clinical trials.

Author contributions

J.H.P., J.Y.S. designed the research studies. N.K.Z., J.F.L.,Y.T.Q. conducted experiments and/or analyzed data. Y.L., J.B.S.,W.H.H. wrote the manuscript and S.G.Z. and Y.M.S. critically reviewed and edited it.

Funding

The study was supported by the Guangdong Basic and Applied Basic Research Foundation (No. 2023A1515140177) to Y Shao, National Natural Science Foundation of China (No. 82072151) to Y Shao, Talent Development Foundation of The First Dongguan Affiliated Hospital of Guangdong Medical University (No. GCC2023005) to Y Shao, Special Project for Clinical and Basic Sci&Tech Innovation of Guangdong Medical University (No. GDMULCJC2024093) to Y Shao.

Conflicts of interest

None declared.

Data availability

All data of this study are available from the corresponding author (S.Y.M.) upon reasonable request.

References

1. Singer M, Deutschman CS, Seymour CW, Shankar-Hari M, Annane D, Bauer M, Bellomo R, et al. The Third International Consensus Definitions for Sepsis and Septic Shock (Sepsis-3). JAMA. 2016; 315:801–810.DOI: 10.1001/jama.2016.0287.

2. Rudd KE, Johnson SC, Agesa KM, Shackelford KA, Tsoi D, Kievlan DR, Colombara DV, et al. Global, regional, and national sepsis incidence and mortality, 1990–2017: analysis for the Global

547 Burden of Disease Study. Lancet. 2020; 395:200–211.DOI: 10.1016/S0140-6736(19)32989-7.

548 3. Wu D, Zhang H, Miao C. The homeostasis and heterogeneity of regulatory T cells in sepsis. Burns
549 Trauma. 2025; 13:tkaf047.DOI: 10.1093/burnst/tkaf047.

550 4. Barichello T, Generoso JS, Singer M, Dal-Pizzol F. Biomarkers for sepsis: more than just fever
551 and leukocytosis—a narrative review. Crit Care. 2022; 26:14.DOI: 10.1186/s13054-021-03862-5.

552 5. Hohlstein P, Gussen H, Bartneck M, Warzecha KT, Roderburg C, Buendgens L, Trautwein C, et
553 al. Prognostic Relevance of Altered Lymphocyte Subpopulations in Critical Illness and Sepsis. J
554 Clin Med. 2019; 8:353.DOI: 10.3390/jcm8030353.

555 6. Inoue S, Suzuki-Utsunomiya K, Okada Y, Taira T, Iida Y, Miura N, Tsuji T, et al. Reduction of
556 immunocompetent T cells followed by prolonged lymphopenia in severe sepsis in the elderly. Crit
557 Care Med. 2013; 41:810–819.DOI: 10.1097/CCM.0b013e318274645f.

558 7. Heffernan DS, Monaghan SF, Thakkar RK, Machan JT, Cioffi WG, Ayala A. Failure to normalize
559 lymphopenia following trauma is associated with increased mortality, independent of the
560 leukocytosis pattern. Crit Care. 2012; 16:R12.DOI: 10.1186/cc11157.

561 8. Ono S, Tsujimoto H, Hiraki S, Aosasa S. Mechanisms of sepsis-induced immunosuppression and
562 immunological modification therapies for sepsis. Ann Gastroenterol Surg. 2018; 2:351–358.DOI:
563 10.1002/ags3.12194.

564 9. Boomer JS, Green JM, Hotchkiss RS. The changing immune system in sepsis. Virulence. 2014;
565 5:45–56.DOI: 10.4161/viru.26516.

566 10. Edwards DR, Handsley MM, Pennington CJ. The ADAM metalloproteinases. Mol Aspects Med.
567 2008; 29:258–289.DOI: 10.1016/j.mam.2008.08.001.

568 11. Zhong S, Khalil RA. A Disintegrin and Metalloproteinase (ADAM) and ADAM with
569 Thrombospondin Motifs (ADAMTS) Family in Vascular Biology and Disease. Biochem Pharmacol.
570 2019; 164:188–204.DOI: 10.1016/j.bcp.2019.03.033.

571 12. Liao S, Lin Y, Liu L, Yang S, Lin Y, He J, Shao Y. ADAM10-a “multitasker” in sepsis: focus on
572 its posttranslational target. Inflamm Res. 2023; 72:395–423.DOI: 10.1007/s00011-022-01673-0.

573 13. Rahn S, Becker-Pauly C. Meprin and ADAM proteases as triggers of systemic inflammation in
574 sepsis. FEBS Lett. 2022; 596:534–556.DOI: 10.1002/1873-3468.14225.

575 14. Cui L, Gao Y, Xie Y, Wang Y, Cai Y, Shao X, Ma X, et al. An ADAM10 promoter polymorphism
576 is a functional variant in severe sepsis patients and confers susceptibility to the development of
577 sepsis. Crit Care. 2015; 19:73.DOI: 10.1186/s13054-015-0796-x.

578 15. Chen F, Wang Y, Zhang W, Cai Y, Zhao T, Mai H, Tao S, et al. A Functional Polymorphism-
579 Mediated Disruption of EGR1/ADAM10 Pathway Confers the Risk of Sepsis Progression. mBio.
580 2019; 10:e01663-19.DOI: 10.1128/mBio.01663-19.

581 16. He J, Zhao T, Liu L, Liao S, Yang S, Lu F, Hong Y, et al. The -172 A-to-G variation in ADAM17
582 gene promoter region affects EGR1/ADAM17 pathway and confers susceptibility to septic mortality
583 with sepsis-3.0 criteria. Int Immunopharmacol. 2022; 102:108385.DOI:
584 10.1016/j.intimp.2021.108385.

585 17. Qin Y, Liao S, Sun J, Ye H, Li J, Pan J, He J, et al. RECK as a Potential Crucial Molecule for
586 the Targeted Treatment of Sepsis. J Inflamm Res. 2025; 18:1787–1813.DOI: 10.2147/JIR.S501856.

587 18. Kleino I, Järviluoma A, Hepojoki J, Huovila AP, Saksela K. Preferred SH3 Domain Partners of
588 ADAM Metalloproteases Include Shared and ADAM-Specific SH3 Interactions. PLoS One. 2015;
589 10:e0121301.DOI: 10.1371/journal.pone.0121301.

590 19. Ebsen H, Lettau M, Kabelitz D, Janssen O. Identification of SH3 Domain Proteins Interacting
591 with the Cytoplasmic Tail of the A Disintegrin and Metalloprotease 10 (ADAM10). PLoS One. 2014;
592 9:e102899.DOI: 10.1371/journal.pone.0102899.

593 20. Bu L, Wang Z, Hu S, Zhao W, Geng X, Zhou T, Zhuo L, et al. Identification of Key mRNAs and
594 lncRNAs in Neonatal Sepsis by Gene Expression Profiling. Comput Math Methods Med. 2020;
595 2020:8741739.DOI: 10.1155/2020/8741739.

596 21. Huang J, Pan Y, Hu G, Sun W, Jiang L, Wang P, Ding X. SRC fine-tunes ADAM10 shedding
597 activity to promote pituitary adenoma cell progression. FEBS J. 2020; 287:190–204.DOI:
598 10.1111/febs.15026.

599 22. Kaur B, Kerbrat J, Kho J, Kaler M, Kanatsios S, Cirillo N. Mechanism-based therapeutic targets
600 of pemphigus vulgaris: A scoping review of pathogenic molecular pathways. Exp Dermatol. 2022;
601 31:154–171.DOI: 10.1111/exd.14453.

602 23. Yang L, Zheng SG. Role of regulatory T cells in inflammatory liver diseases. Autoimmun Rev.
603 2025; 24:103806.DOI: 10.1016/j.autrev.2025.103806.

24. Zhang X, Olsen N, Zheng SG. The progress and prospect of regulatory T cells in autoimmune diseases. J Autoimmun. 2020; 111:102461.DOI: 10.1016/j.jaut.2020.102461.

25. Savage PA, Klawon DEJ, Miller CH. Regulatory T Cell Development. Annu Rev Immunol. 2020; 38:421–453.DOI: 10.1146/annurev-immunol-100219-020937.

26. Gao Y, Yao Y, Zhang X, Chen F, Meng X, Chen X, Wang C, et al. Regulatory T Cells: Angels or Demons in the Pathophysiology of Sepsis? Front Immunol. 2022; 13:829210.DOI: 10.3389/fimmu.2022.829210.

27. Okeke EB, Okwor I, Mou Z, Jia P, Uzonna JE. CD4+CD25+ regulatory T cells attenuate lipopolysaccharide-induced systemic inflammatory responses and promotes survival in murine Escherichia coli infection. Shock. 2013; 40:65–73.DOI: 10.1097/SHK.0b013e318296e65b.

28. Jiang W, Li X, Ding H, Wang K, Liu X, Wang Q, Li Y, et al. PD-1 in Tregs predicts the survival in sepsis patients using sepsis-3 criteria: A prospective, two-stage study. Int Immunopharmacol. 2020; 89:107175.DOI: 10.1016/j.intimp.2020.107175.

29. Carvelli J, Piperoglou C, Bourenne J, Farnarier C, Banzet N, Demerlé C, Gainnier M, et al. Imbalance of Circulating Innate Lymphoid Cell Subpopulations in Patients With Septic Shock. Front Immunol. 2019; 10:2179.DOI: 10.3389/fimmu.2019.02179.

30. Liu Q, An L, Qi Z, Zhao Y, Li C. Increased Expression of Programmed Cell Death-1 in Regulatory T Cells of Patients with Severe Sepsis and Septic Shock: An Observational Clinical Study. Scand J Immunol. 2017; 86:408–417.DOI: 10.1111/sji.12612.

623 31. Wu H-P, Chung K, Lin C-Y, Jiang B-Y, Chuang D-Y, Liu Y-C. Associations of T helper 1, 2, 17
624 and regulatory T lymphocytes with mortality in severe sepsis. Inflamm Res. 2013; 62:751–763.DOI:
625 10.1007/s00011-013-0630-3.

626 32. Zhang X, Chen Y, Ling Y, Wu L, Liu D, Wang L, Liu Y, et al. Infusion of Induced Regulatory T
627 Cells Alleviates Atherosclerosis by Reducing Pathological Macrophage-Like Vascular Smooth
628 Muscle Cells. MedComm (2020). 2025; 6:e70439.DOI: 10.1002/mco2.70439.

629 33. Cajander S, Kox M, Scicluna BP, Weigand MA, Mora RA, Flohé SB, Martin-Loeches I, et al.
630 Profiling the dysregulated immune response in sepsis: overcoming challenges to achieve the goal
631 of precision medicine. Lancet Respir Med. 2024; 12:305–322.DOI: 10.1016/S2213-
632 2600(23)00330-2.

633 34. Hotchkiss RS, Karl IE. The pathophysiology and treatment of sepsis. N Engl J Med. 2003;
634 348:138–150.DOI: 10.1056/NEJMra021333.

635 35. van der Poll T, Shankar-Hari M, Wiersinga WJ. The immunology of sepsis. Immunity. 2021;
636 54:2450–2464.DOI: 10.1016/j.immuni.2021.10.012.

637 36. Cinel I, Opal SM. Molecular biology of inflammation and sepsis: a primer. Crit Care Med. 2009;
638 37:291–304.DOI: 10.1097/CCM.0b013e31819267fb.

639 37. Liu D, Huang S-Y, Sun J-H, Zhang H-C, Cai Q-L, Gao C, Li L, et al. Sepsis-induced
640 immunosuppression: mechanisms, diagnosis and current treatment options. Mil Med Res. 2022;
641 9:56.DOI: 10.1186/s40779-022-00422-y.

642 38. Wan YY. Regulatory T cells: immune suppression and beyond. Cell Mol Immunol. 2010; 7:204–
643 210.DOI: 10.1038/cmi.2010.20.

644 39. Askenasy N. Enhanced killing activity of regulatory T cells ameliorates inflammation and
645 autoimmunity. Autoimmun Rev. 2013; 12:972–975.DOI: 10.1016/j.autrev.2013.04.005.

646 40. Li X, Mai J, Virtue A, Yin Y, Gong R, Sha X, Gutchigian S, et al. IL-35 Is a Novel Responsive
647 Anti-inflammatory Cytokine — A New System of Categorizing Anti-inflammatory Cytokines.
648 PLoS One. 2012; 7:e33628.DOI: 10.1371/journal.pone.0033628.

649 41. Vignali DAA, Kuchroo VK. IL-12 Family Cytokines: Immunological Playmakers. Nat Immunol.
650 2012; 13:722–728.DOI: 10.1038/ni.2366.

651 42. Nascimento DC, Melo PH, Piñeros AR, Ferreira RG, Colón DF, Donate PB, Castanheira FV, et
652 al. IL-33 contributes to sepsis-induced long-term immunosuppression by expanding the regulatory
653 T cell population. Nat Commun. 2017; 8:14919.DOI: 10.1038/ncomms14919.

654 43. Collison LW, Delgoffe GM, Guy CS, Vignali KM, Chaturvedi V, Fairweather D, Satoskar AR,
655 et al. The composition and signaling of the IL-35 receptor are unconventional. Nat Immunol. 2012;
656 13:290–299.DOI: 10.1038/ni.2227.

657 44. Ammirati E, Cianflone D, Banfi M, Vecchio V, Palini A, De Metrio M, Marenzi G, et al.
658 Circulating CD4+CD25hiCD127lo regulatory T-Cell levels do not reflect the extent or severity of
659 carotid and coronary atherosclerosis. Arterioscler Thromb Vasc Biol. 2010; 30:1832–1841.DOI:
660 10.1161/ATVBAHA.110.206813.

661 45. Zeng C, Shi X, Zhang B, Liu H, Zhang L, Ding W, Zhao Y. The imbalance of Th17/Th1/Tregs
662 in patients with type 2 diabetes: relationship with metabolic factors and complications. J Mol Med
663 (Berl). 2012; 90:175–186.DOI: 10.1007/s00109-011-0816-5.

664 46. Alvarado-Sánchez B, Hernández-Castro B, Portales-Pérez D, Baranda L, Layseca-Espinosa E,
665 Abud-Mendoza C, Cubillas-Tejeda AC, et al. Regulatory T cells in patients with systemic lupus
666 erythematosus. J Autoimmun. 2006; 27:110–118.DOI: 10.1016/j.jaut.2006.06.005.

667 47. Möttönen M, Heikkinen J, Mustonen L, Isomäki P, Luukkainen R, Lassila O. CD4+ CD25+ T
668 cells with the phenotypic and functional characteristics of regulatory T cells are enriched in the
669 synovial fluid of patients with rheumatoid arthritis. Clin Exp Immunol. 2005; 140:360–367.DOI:
670 10.1111/j.1365-2249.2005.02754.x.

671 48. Xiong Z, Song J, Yan Y, Huang Y, Cowan A, Wang H, Yang X-F. Higher expression of Bax in
672 regulatory T cells increases vascular inflammation. Front Biosci. 2008; 13:7143–7155.DOI:
673 10.2741/3217.

674 49. Yang X-F, Weber GF, Cantor H. A Novel Bcl-x Isoform Connected to the T Cell Receptor
675 Regulates Apoptosis in T Cells. Immunity. 1997; 7:629–639.DOI: 10.1016/s1074-7613(00)80384-
676 2.

677 50. Zheng SG, Wang J, Wang P, Gray JD, Horwitz DA. IL-2 is essential for TGF-beta to convert
678 naive CD4+CD25- cells to CD25+Foxp3+ regulatory T cells and for expansion of these cells. J
679 Immunol. 2007; 178:2018–2027.DOI: 10.4049/jimmunol.178.4.2018.

680 51. Ye C, Brand D, Zheng SG. Targeting IL-2: an unexpected effect in treating immunological

681 diseases. Signal Transduct Target Ther. 2018; 3:2.DOI: 10.1038/s41392-017-0002-5.

682 52. Davidson TS, DiPaolo RJ, Andersson J, Shevach EM. Cutting Edge: IL-2 is essential for TGF-
683 beta-mediated induction of Foxp3+ T regulatory cells. J Immunol. 2007; 178:4022–4026.DOI:
684 10.4049/jimmunol.178.7.4022.

685 53. Flemming S, Burkard N, Renschler M, Vielmuth F, Meir M, Schick MA, Wunder C, et al.
686 Soluble VE-cadherin is involved in endothelial barrier breakdown in systemic inflammation and
687 sepsis. Cardiovasc Res. 2015; 107:32–44.DOI: 10.1093/cvr/cvv144.

688 54. Deng W, Cho S, Su P-C, Berger BW, Li R. Membrane-enabled dimerization of the intrinsically
689 disordered cytoplasmic domain of ADAM10. Proc Natl Acad Sci U S A. 2014; 111:15987–
690 15992.DOI: 10.1073/pnas.1409354111.

691 55. Huang J, Pan Y, Hu G, Sun W, Jiang L, Wang P, Ding X. SRC fine-tunes ADAM10 shedding
692 activity to promote pituitary adenoma cell progression. FEBS J. 2020; 287:190–204.DOI:
693 10.1111/febs.15026.

694 56. Matthews AL, Koo CZ, Szyroka J, Harrison N, Kanhere A, Tomlinson MG. Regulation of
695 Leukocytes by TspanC8 Tetraspanins and the 'Molecular Scissor' ADAM10. Front Immunol. 2018;
696 9:1451.DOI: 10.3389/fimmu.2018.01451.

697 57. Carter JD, Calabrese GM, Naganuma M, Lorenz U. Deficiency of the Src homology region 2
698 domain-containing phosphatase 1 (SHP-1) causes enrichment of CD4+CD25+ regulatory T cells. J
699 Immunol. 2005; 174:6627–6638.DOI: 10.4049/jimmunol.174.11.6627.

700 58. Sharabi A, Li H, Kasper IR, Pan W, Meidan E, Tsokos MG, Moulton VR, et al. PP2A enables
701 IL-2 signaling by preserving IL-2Rβ chain expression during Treg development. JCI Insight. 2019;
702 5:e126294, 126294.DOI: 10.1172/jci.insight.126294.

703 59. Lowe DB, Bose A, Taylor JL, Tawbi H, Lin Y, Kirkwood JM, Storkus WJ. Dasatinib promotes
704 the expansion of a therapeutically superior T-cell repertoire in response to dendritic cell vaccination
705 against melanoma. Oncoimmunology. 2014; 3:e27589.DOI: 10.4161/onci.27589.

706 60. Rabenau KE, Dolan M, Yohe S, Ustun C. Effectiveness of dasatinib in accelerated-phase chronic
707 myeloid leukemia with p190 BCR-ABL1 and a second Philadelphia chromosome. Cancer Genet.
708 2014; 207:109–110.DOI: 10.1016/j.cancergen.2014.02.006.

709 61. Fraser CK, Lousberg EL, Kumar R, Hughes TP, Diener KR, Hayball JD. Dasatinib inhibits the
710 secretion of TNF-alpha following TLR stimulation in vitro and in vivo. Exp Hematol. 2009;
711 37:1435–1444.DOI: 10.1016/j.exphem.2009.09.007.

712 62. Oliveira GP, Silva JD, Marques PS, Gonçalves-de-Albuquerque CF, Santos HL, Vascocellos AP,
713 Takiya CM, et al. The Effects of Dasatinib in Experimental Acute Respiratory Distress Syndrome
714 Depend on Dose and Etiology. Cell Physiol Biochem. 2015; 36:1644–1658.DOI:
715 10.1159/000430325.

716 63. Yang X-F. Factors regulating apoptosis and homeostasis of CD4+ CD25(high) FOXP3+
717 regulatory T cells are new therapeutic targets. Front Biosci. 2008; 13:1472–1499.DOI:
718 10.2741/2775.

719 64. Pierson W, Cauwe B, Policheni A, Schlenner SM, Franckaert D, Berges J, Humblet-Baron S, et

al. Anti-apoptotic Mcl-1 is critical for the survival and niche-filling capacity of Foxp3+ regulatory T cells. Nat Immunol. 2013; 14:959–965.DOI: 10.1038/ni.2649.

Authors and Affiliations

Jiahui Pan[1,2,3,4] · Junyi Shao[2,4] · Nianke Zang[2] · Jiafu Li[2,3,4] · Yuting Qin[2,3,4] · Yu Liu[2] · Jianbo Sun[2,5] · Wenhong Hou[2] · Song Guo Zheng[2,6,7*] · Yiming Shao[2,4*]

Dr. Yiming Shao

sym@gdmu.edu.cn.

Song Guo Zheng

Song.Zheng@shsmu.edu.cn.

[1]School of Medical Technology, Guangdong Medical University, Zhanjiang 524023, China

[2]The First Dongguan Affiliated Hospital, Guangdong Medical University, Dongguan 523710, China

[3]The Intensive Care Unit, The First Dongguan Affiliated Hospital, Guangdong Medical University, Dongguan 523710, China

[4]Dongguan Key Laboratory of Sepsis Translational Medicine, Guangdong, Dongguan 523710, China

[5]Dongguan Key Laboratory of Chronic Inflammatory Diseases, Dongguan 523710, China

[6]Department of Immunology, School of Cell and Gene Therapy, Songjiang Research Institute, Shanghai Songjiang District Central Hospital, Shanghai Jiao Tong University School of Medicine, Shanghai 201600, China

[7]State Key Laboratory of Innovative Immunotherapy, Shanghai Jiao Tong University, Shanghai 201600, China

* Corresponding author.